

AdaptSky: A DRL Based Resource Allocation Framework in NOMA-UAV Networks

Ahmed Benfaid*, Nadia Adem*, and Bassem Khalfi**

*University of Tripoli, Tripoli, Libya, Email: {a.benfaid,n.adem}@uot.edu.ly

**Qualcomm Technologies Inc., CA, USA, Email: bkhalfi@qti.qualcomm.com

Abstract—Unmanned aerial vehicle (UAV) has recently attracted a lot of attention as a candidate to meet the 6G ubiquitous connectivity demand and boost the resiliency of terrestrial networks. Thanks to the high spectral efficiency and low latency, non-orthogonal multiple access (NOMA) is a potential access technique for future communication networks. In this paper, we propose to use the UAV as a moving base station (BS) to serve multiple users using NOMA and jointly solve for the 3D-UAV placement and resource allocation problem. Since the corresponding optimization problem is non-convex, we rely on the recent advances in artificial intelligence (AI) and propose AdaptSky, a deep reinforcement learning (DRL)-based framework, to efficiently solve it. To the best of our knowledge, AdaptSky is the first framework that optimizes NOMA power allocation jointly with 3D-UAV placement using both sub-6GHz and millimeter wave mmWave spectrum. Furthermore, for the first time in NOMA-UAV networks, AdaptSky integrates the dueling network (DN) architecture to the DRL technique to improve its learning capabilities. Our findings show that AdaptSky does not only exhibit a fast-adapting learning and outperform the state-of-the-art baseline approach in data rate and fairness, but also it generalizes very well.

Index Terms—3D networks, deep reinforcement learning (DRL), dueling network (DN) architecture, millimeter wave (mmWave), non-orthogonal multiple access (NOMA), unmanned aerial vehicle (UAV).

I. INTRODUCTION

Future communication networks are envisioned to provide heterogeneous wireless communication services with significant performance boost over 5G networks [1]. Unmanned aerial vehicles (UAVs), artificial intelligence (AI), millimeter wave (mmWave), along with some emerging medium access techniques are very key technologies in meeting such a goal [2]. For instance, thanks to their flexible 3D mobility, ease of deployment, and location precision, UAVs can serve as aerial base stations (BSs), and hence, augment or replace terrestrial BSs in some extreme scenarios [3]. Hence, it has become an active topic for different working groups in standardization bodies such as 3GPP [4].

Rendering to its ability to simultaneously share spectrum resources among multiple users, non-orthogonal multiple access (NOMA) promises for massive-devices connectivity making it a candidate access technique for beyond 5G systems. Moreover, when used in mmWave spectrum, NOMA offers a significant data rate boost. Nevertheless, efficiently managing resources for mmWave or even sub-6GHz spectrum for NOMA-UAV networks with a heterogeneous number of users is a complex problem [5]. In this perspective, we propose

a novel advanced deep reinforcement learning (DRL)-based framework that solves jointly for the UAV placement and NOMA resource allocation in the context of sub-6GHz as well as mmWave spectrum.

A. Related Work

There are few works available about NOMA-UAV networks, some of which have focused on UAV placement and NOMA resources (mostly power) allocation, for example [6]–[9]. The issues, however, with these works that, for simplicity they *i*) assume links between users and UAVs are dominated by line-of-sight (LoS), as it is the case with [6]–[8], *ii*) restrict the number of users in the network to two, e.g. [7], [9], *iii*) solve for UAV placement and NOMA power allocation disjointly, for example [6], and/or *iv*) limit the UAV analysis to 2D placement, e.g. [6]–[9]. There have been some attempts in handling the 3D-placement problem of UAV such as in [10]–[12]. Yet, these works optimize the altitude and the 2D-UAVs placement disjointly. Imposing restrictions in analyzing 3D networks, can lead to inefficient use of resources. Hence, some innovative techniques that can handle their analysis complexity are needed.

A remarkable success has been reported from incorporating DRL into the field of gaming [13]. DRL, which is mainly a reinforcement learning (RL) technique combined with deep-neural-network (DNN), has the potential to handle high-dimensional inputs, learn patterns, and solve complex problems efficiently [13], [14]. Even though some initial works consider DRL for 2D-UAVs placement in the presence of LoS links only e.g. [15], the full potentials of DRL for 3D networks still need to be assessed. We aim, in this paper, to solve the non-convex optimization problem of the 3D-network resources management using recent advances in DRL.

B. Key Contributions

In this paper, we aim to bring forth the most-recent advances in AI to efficiently solve the UAV placement and resources management while maximizing both users data rate and fairness. Our main contributions are summarized as follows

- 1) We propose a unified model-free framework, AdaptSky, for UAV placement and power allocation in a NOMA-based 3D network. We integrate dueling network with DRL, for the first time in NOMA-UAV networks, and demonstrate the tremendous-gain resultant in learning model generalization, and hence, network performance.

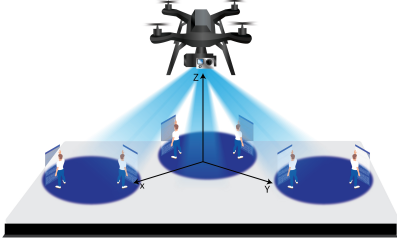


Fig. 1: UAV communication network environment

- 2) We show that AdaptSky is robust for different path loss models both for the sub-6GHz and mmWave spectrum.
- 3) We show that AdaptSky maximizes the spectral efficiency while maintaining high users' fairness. Simulation results shows that AdaptSky outperforms legacy baseline approach.

C. Roadmap

The rest of this paper is organized as follows. The system model and problem formulation are presented in Section II and III, respectively. AdaptSky framework is proposed and discussed in Section IV. In Section V, we provide the simulation results. Finally, we present the conclusion in Section VI.

II. SYSTEM MODEL

A. Network Model

We consider a downlink cellular network with a UAV serving $N_{\text{UE}} = 2N$ ground users distributed randomly over an area \mathcal{A} of $L \times L$ units and grouped into a number of clusters as shown by Fig. 1. To get the most out of NOMA, two users with distinct channel qualities get associated to a single cluster based on the strategy proposed in [5]. The UAV serves each cluster over an orthogonal resource with a total power P_T distributed between the two corresponding users. The UAV is also assumed to be equipped with \mathcal{N}_{UAV} antennas while each user is equipped with \mathcal{N}_{UE} antennas, unless specified otherwise. Throughout the paper, user i is denoted by UE_i where $i \in \{1, 2, \dots, N_{\text{UE}}\}$. Without loss of generality, we assume that the users UE_i and UE_{i+1} for $i \in \{1, 3, \dots, N_{\text{UE}} - 1\}$ are associated with the same cluster and UE_i has a stronger channel gain than UE_{i+1} .

The received power at the UE_i at a given time step τ can be expressed as

$$\hat{P}_{i,\tau} = P_T \ell_{i,\tau}^{\text{MIMO}}(d_{i,\tau}) \alpha_{i,\tau}, \quad (1)$$

where $\ell_{i,\tau}^{\text{MIMO}}(d_{i,\tau})$ is the path loss gain between the UAV and UE_i separated, at τ , by a 3D distance $d_{i,\tau}$. Considering only a large scale fading (small scale fading is deferred for future works) and assuming a slight difference between antenna pairs, the loss can be approximated as $\ell_{i,\tau}^{\text{MIMO}}(d_{i,\tau}) = G \ell_{i,\tau}(d_{i,\tau})$, where $G = \mathcal{N}_{\text{UAV}} \times \mathcal{N}_{\text{UE}}$. $\ell_{i,\tau}(d_{i,\tau})$ is the path gain between one UAV- UE_i antenna pair. $\alpha_{i,\tau}$ is the power allocation coefficient that determines the amount of power (out of P_T) the UAV assigns

to UE_i at the time step τ . Also $\alpha_{i,\tau} + \alpha_{i+1,\tau} = 1 \forall i \in \{1, 3, \dots, N_{\text{UE}} - 1\}$. The 3D distance $d_{i,\tau}$ between the UAV located at $(x_{\text{UAV},\tau}, y_{\text{UAV},\tau}, h_{\text{UAV},\tau})$ and UE_i located at $(x_{i,\tau}, y_{i,\tau}, 0)$ at time step τ is given by

$$d_{i,\tau} = \sqrt{h_{\text{UAV},\tau}^2 + (x_{\text{UAV},\tau} - x_{i,\tau})^2 + (y_{\text{UAV},\tau} - y_{i,\tau})^2}. \quad (2)$$

B. Signal-to-Interference-plus-Noise Ratio (SINR)

Following the NOMA protocol, the superposition coding (SC) is used at the UAV to transmit messages for users located in the same cluster. SC encodes different messages into a single signal while assigning them different power values. The successive interference cancellation (SIC) is used at the receiver side for signal detection. The received SINR at UE_i is expressed as

$$\text{SINR}_{i,\tau} = \frac{P_T \times \ell_{i,\tau}(d_{i,\tau}) \times G \times \alpha_{i,\tau}}{P_T \times \ell_{i,\tau}(d_{i,\tau}) \times G \times \beta_{i,\tau} + \sigma^2}, \quad (3)$$

where $\beta_{i,\tau} = \alpha_{i-1,\tau}$ if i is even and zero otherwise. σ^2 is the noise power. The first term in the denominator of equation (3) represents the interference from the user with the best channel condition to the other user. Based on the SIC technique, however, the interference at the user with the best channel condition gets canceled, which is the intuition behind the definition of $\beta_{i,\tau}$. For a bandwidth W , the data rate of UE_i at τ is given by

$$R_{i,\tau} = W \log_2(1 + \text{SINR}_{i,\tau}). \quad (4)$$

C. Channel Model

We consider to explore the performance of our system in both mmWave and sub-6GHz spectrum in the presence of the LoS and NLoS links. Throughout, we present the path loss definition for mmWave as well as the sub-6GHz. To accommodate for the various links and spectrum technologies, we modify the path loss gain notation to be $\ell_{i,\tau}^{k,sp}(d_{i,\tau})$, where $k \in \{\text{LoS}, \text{NLoS}\}$ and $sp \in \{\text{mmWave}, \text{sub-6}\}$.

1) *MmWave Channel Model*: Following the same model as in [16], at time step τ , the UAV- UE_i link is assumed to be in LoS with a probability $Pr_{i,\tau}^{\text{LoS},\text{mmWave}}(\theta_{i,\tau})$ given as

$$Pr_{i,\tau}^{\text{LoS},\text{mmWave}}(\theta_{i,\tau}) = \frac{1}{1 + C \exp[-Y(\theta_{i,\tau} \frac{180}{\pi} - C)]}, \quad (5)$$

where C and Y are environment parameters, $\theta_{i,\tau}$ is the elevation angle ($\arcsin(\frac{h_{\text{UAV},\tau}}{d_{i,\tau}})$) between the UAV and UE_i at time step τ . Similarly, UE_i is assumed to be in NLoS using the complement property, i.e., $Pr_{i,\tau}^{\text{NLoS},\text{mmWave}}(\theta_{i,\tau}) = 1 - Pr_{i,\tau}^{\text{LoS},\text{mmWave}}(\theta_{i,\tau})$. The path loss gain equation $\ell_{i,\tau}^{k,\text{mmWave}}(d_{i,\tau})$ between the UAV located at a distance $d_{i,\tau}$ from UE_i , according to [17] is expressed as

$$\ell_{i,\tau}^{k,\text{mmWave}}(d_{i,\tau}) = C_k d_{i,\tau}^{-a_k}, \quad (6)$$

where a_k is the path loss exponent, and C_k is the unit distance path loss gain.

2) *Sub-6GHz Channel Model*: Similar to [18], UE_i is assumed to be in LoS with a probability of $P_{r_{i,\tau}}^{\text{LoS},\text{sub-6}}(\theta_{i,\tau})$ defined as

$$P_{r_{i,\tau}}^{\text{LoS},\text{sub-6}}(\theta_{i,\tau}) = b.(\theta_{i,\tau} - \theta_0)^s, \quad (7)$$

where b and s are frequency and environment dependent parameters. θ_0 is the minimum angle allowed by the model. Similarly, UE_i is assumed to be in NLoS using the complement property $P_{r_{i,\tau}}^{\text{NLoS},\text{sub-6}}(\theta_{i,\tau}) = 1 - P_{r_{i,\tau}}^{\text{LoS},\text{sub-6}}(\theta_{i,\tau})$. The path gain for the UE_i is defined as

$$\ell_{i,\tau}^{k,\text{sub-6}}(d_{i,\tau}) = \left(\frac{c}{4\pi f_c d_{i,\tau}}\right)^2 10^{-0.1\eta_k}, \quad (8)$$

where f_c is the carrier frequency, and $\left(\frac{c}{4\pi f_c d_{i,\tau}}\right)^2$ represents the free space path loss gain. η_k , measured in dB, is the mean additional loss for k th (LoS or NLoS) transmission link as defined in [18].

D. UAV Mobility Model

At time step τ , the UAV is assumed to be placed at $(x_{\text{UAV},\tau}, y_{\text{UAV},\tau}, h_{\text{UAV},\tau})$ and able to move to $(x_{\text{UAV},\tau} + d_x\delta_x, y_{\text{UAV},\tau} + d_y\delta_y, h_{\text{UAV},\tau} + d_h\delta_h)$, where d_x, d_y , and $d_h \in \{1, -1\}$. δ_x , and δ_y are the magnitude of change in the x and y axis, respectively. δ_h is the magnitude of change in the height. The UAV height, at any time step, is assumed to be higher than a height of h_0 . We assume that at an initial time step τ_0 , the UAV is deployed in the middle of the coverage area \mathcal{A} with an initial height h_{UAV,τ_0} , i.e., located at $(0, 0, h_{\text{UAV},\tau_0})$. Without loss of generality, we assume the UAV can collect the channel state information (CSI) at the beginning of each time step [19].

III. 3D-UAV PLACEMENT AND POWER ALLOCATION FORMULATION

We propose to optimize the UAV placement and power allocation that maximizes the total users' data rate and fairness. First, we define the sum users' data rate at time step τ as

$$R_\tau^{\text{tot}} = \sum_{i=1}^{N_{\text{UE}}} W \log_2(1 + \text{SINR}_{i,\tau}), \quad (9)$$

and, using the Jain's fairness index [20], the users' fairness as

$$J_\tau^f = \frac{(\sum_{i=1}^{N_{\text{UE}}} R_{i,\tau})^2}{N_{\text{UE}} \sum_{i=1}^{N_{\text{UE}}} R_{i,\tau}^2}. \quad (10)$$

The optimization problem is formulated as the following

$$\max_{x_{\text{UAV},\tau}, y_{\text{UAV},\tau}, h_{\text{UAV},\tau}, \alpha_{i,\tau}} \omega_r \times R_\tau^{\text{tot}} + \omega_f \times J_\tau^f, \quad (11a)$$

$$\alpha_{i,\tau} > 0, \forall i \in \{1, \dots, N_{\text{UE}}\}, \quad (11b)$$

$$\alpha_{i,\tau} + \alpha_{i+1,\tau} = 1, \forall i \in \{1, 3, \dots, N_{\text{UE}} - 1\}, \quad (11c)$$

$$R_{i,\tau} \geq R_{\text{min}}, \forall i \in \{1, \dots, N_{\text{UE}}\}, \quad (11d)$$

$$L/2 \geq x_{\text{UAV},\tau} \geq -L/2, \quad (11e)$$

$$L/2 \geq y_{\text{UAV},\tau} \geq -L/2, \quad (11f)$$

$$h_{\text{UAV},\tau} \geq h_0, \quad (11g)$$

$$\omega_r \geq 0, \omega_f \geq 0, \quad (11h)$$

where R_{min} is a minimum required rate for each user.

Remark 1: To guarantee the feasibility of the problem at hand, the power allocation should satisfy:

$2^{(-R_{\text{min}}/W)} > \alpha_{i,\tau}$, for $i \in \{1, 3, \dots, N_{\text{UE}} - 1\}$, which follows from (11d).

The objective function in (11) is not convex, hence finding the optimal power allocation and UAV placement is challenging. Note that an optimal solution should strike a balance between two conflicting objectives: maximizing total users' data rate and users' fairness. These two objectives vary drastically based on users-to-UAV 3D distances, environment, and spectrum. Inspired by the recent advances and success of deep reinforcement learning, we propose an efficient framework allows the UAV to learn fast how to maximize objectives, satisfy requirements, learn environment patterns, and adapt to related-unseen environments, and hence provides the best solution for (11).

IV. AdaptSky: A DRL-BASED MODEL FOR RESOURCE ALLOCATION AND UAV PLACEMENT

A. Preliminaries

Before getting into our proposed framework, we give a necessary background about the the RL, DRL, and the DN architecture. In the RL literature, an agent in a state, s_τ , performs an action a_τ that allows it to move to another state $s_{\tau+1}$, and receives a reward r_τ at each time based on Bellman equation [21]. RL is an optimization technique that helps finding the optimal policy π_* , which is a series of actions, that leads the agent to optimize a certain objective, say a total discounted reward $r^{\text{tot}} = \sum_{\tau=0}^T \gamma^\tau r_\tau$, where γ is a discount factor, and T is the total number of time steps. In spite of the fact that the RL method has been successful in solving certain problems in wireless communication, RL falls short in handling environments represented by continuous state space. The computational resources and time required for the iterative process of updating the table in a large state space makes the RL inefficient for solving many optimization problems. Fortunately, this can be addressed using DNNs, which does not have to iterate over each set of state-action pairs but rather learn the pattern that maximizes the total reward. The DNN approximates the Q-values for each action taken from a given input state with the aim of approximating the ideal Q-function that satisfies Bellman equation:

$$Q_*(s_\tau, a_\tau) = \mathbb{E} \left[r_\tau + \gamma \max_{a_{\tau+1}} Q_*(s_{\tau+1}, a_{\tau+1}) \right] \quad (12)$$

where $Q_*(s_{\tau+1}, a_{\tau+1})$ is the optimal Q-value for the next state-action pair $(s_{\tau+1}, a_{\tau+1})$. The DNN is trained by minimizing the following loss function

$$L(\theta^\pi) = \mathbb{E}[r_\tau + \gamma Q(s_{\tau+1}, a_{\tau+1}; \theta'^\pi) - Q(s_\tau, a_\tau; \theta^\pi)] \quad (13)$$

where θ^π and θ'^π are the weights of the policy and target network, respectively. Since DNN may cause instability or divergence, DRL solves this by using experience replay. Instead of using the immediately collected sample, DRL uses a mini-batch from an experience replay buffer that stores $s_\tau, a_\tau, s_{\tau+1}$ and r_τ each time step and randomly samples a mini-batch

during the learning to calculate the loss and updates the DNN. This is referred to as policy network. Note that in Eq. (13), if $Q_*(s_{\tau+1}, a_{\tau+1}; \theta^\pi)$ is computed using the same *policy network* that the agent is taking actions from, the DNN will never learn. So, another network is needed to estimate the next Q-value which is named the *target network*. It is a replica of the policy network with frozen weights and biases to the policy network's weights and biases for certain time steps, then the target network's weights and biases are changed to the policy network's current weights and biases every δ time steps.

B. AdaptSky: DRL-based Framework

We propose AdaptSky which is a DRL-based framework that allows the UAV to efficiently position in a 3D plane while efficiently serving the different users. AdaptSky helps solve the optimization problem defined in (11). We start by formally defining the states, actions, and rewards as follows.

- 1) **States.** At time step τ , the state s_τ describes the relative locations of the UAV and users, all users power coefficient, and UAV-UE_i path loss gain. s_τ is defined as $s_\tau = [s_{1,\tau}^T, s_{2,\tau}^T, \dots, s_{N_{UE},\tau}^T, h_\tau]^T$ where $s_{i,\tau} = [\Delta x_{UAV-i,\tau}, \Delta y_{UAV-i,\tau}, \alpha_{i,\tau}, \ell_{i,\tau}(d_{i,\tau})]^T$ where $\Delta x_{UAV-i,\tau}$ is the step distance between the UAV and UE_i in the x-axis, $\Delta y_{UAV-i,\tau}$ is the step distance between the UAV and UE_i in the y-axis, and h_τ is the UAV current height. The cardinality of s_τ is $(4 \times N_{UE} + 1)$.
- 2) **Actions.** The actions are defined as $a_\tau = [d_x \delta_x, d_y \delta_y, d_h \delta_h, \delta_\alpha^T]^T$ where δ_α is defined as $[d_1 \delta_1, d_3 \delta_3, \dots, d_{N_{UE}-1} \delta_{N_{UE}-1}]^T$, $d_i \in \{1, -1\}$ and δ_i is the magnitude of change in the power allocation coefficient of the UE_i $\forall i \in \{1, 3, \dots, N_{UE} - 1\}$. The power coefficients of the other users are derived as described in section (II). a_τ determines the adjustments the UAV needs to make in its 3D placement and the power allocated to all users. The action vector has a cardinality of $(3 + N_{UE}/2)$.
- 3) **Rewards.** We define the reward at time step τ as

$$r_\tau = w_r \times R_\tau^{\text{tot}} + w_f \times J_\tau^f + w_l \times \ell_\tau^{\text{tot}} + w_m \times \sum_{i=1:N_{UE}} \mathbb{1}(R_{i,\tau} \geq R_{\min}), \quad (14)$$

where ℓ_τ^{tot} defines the total users path loss gain. $\mathbb{1}(\cdot)$ is the indicator function. w_r, w_f, w_l , and w_m are the weights corresponding to the rate, fairness, loss and minimum rate rewards, respectively. While the loss reward helps in learning patterns, the last term in the reward function reinforces for satisfying the minimum rate requirement. The weights can change depending on the objective.

Having described the different states, actions, and rewards, we now present AdaptSky as in Algorithm 1. Initially, a replay memory ζ with a capacity M is initialized. Whenever ζ reaches its full capacity M , a new experience replaces the old one so that the new observed experiences are stored. Also the policy network Q weights and biases are initialized to random values. To improve the learning stability, a target

network Q' is used, which has the same structure as Q , and we clone the policy network parameters to the target network by making $\theta'^\pi = \theta^\pi$. At the beginning of each episode, AdaptSky resets the environment and receives the starting state s_0 and pre-processes the starting state ϕ_0 . As shown in step 6 on-wards in Algorithm 1, the UAV selects and executes an action according to ϵ -greedy strategy which balances exploration and exploitation. After executing a_τ , the UAV observes the reward r_τ , then updates the state $s_\tau = s_{\tau+1}$ and pre-processes it as before, $\phi_{\tau+1} = \phi(s_{\tau+1})$. After that, everything is stored in ζ . Then, a mini-batch of B is sampled from ζ and used to train the policy network.

Implementation details. The mini-batch size B is set to 128 and the maximum capacity $M = 15,000$, then we calculate Q-values from Q and the target Q-values from Q' and calculate the loss $L(\theta^\pi)$. After that, we minimize the loss $L(\theta^\pi)$ by updating the policy network weights and biases θ^π using Adam optimizer [22], which is adapted to noisy problems with sparse gradients. After 10 time steps, AdaptSky updates the target network weights and biases to the policy network weights and biases, $\theta'^\pi = \theta^\pi$. AdaptSky network consists of 2 fully-connected layers of 128 neurons each, and uses the ReLU as an activation function. We also rely on dueling network (DN) architecture which shows a good improvement in the learning process and speed [23]. We further define an important quantity in DN architecture, named the advantage function defined as $A(s_\tau, a_\tau) = Q(s_\tau, a_\tau) - V(s_\tau)$ where $V(s_\tau) = \mathbb{E}_{a_\tau \sim \pi(s_\tau)}[Q(s_\tau, a_\tau)]$, where value function V measures how good it is to be in a particular state s_τ while the Q function measures the value of choosing a particular action when in this state. One of the advantages of the DN architecture is its ability to learn the state-value function efficiently. In the DN architecture, the value V is updated with every update of the Q values, unlike in traditional architectures, where only the value for one of the actions is changed.

V. AdaptSky PERFORMANCE EVALUATION

A. Simulation Settings

AdaptSky performance is tested for a 100×100 m^2 area \mathcal{A} with $N_{UE} = 4$ divided into 2 clusters. Users UE₁ and UE₂ are assumed to belong to the same cluster based on their locations. The Cartesian coordinates of the users are set to $(x_1, y_1) = (4, 15)$, $(x_2, y_2) = (-44, -49)$, $(x_3, y_3) = (-5, 21)$ and $(x_4, y_4) = (47, 49)$, unless specified otherwise. The minimum UAV height h_{\min} is set to 10 m. At the beginning of each episode, the initial height of the UAV is $h_{UAV,0} = 50$ m and it can move with $\delta d_{UAV} = \sqrt{(\delta_x)^2 + (\delta_y)^2} = \sqrt{2}$ m, and $\delta_h = 1$ m each time step. The channel is modeled according to [17] which provides the New York city model. All related channel model parameters are shown in Table I.

B. Numerical Analysis

We use Python 3.8.5 with PyTorch library 1.7.1 on an Intel(R) Core(TM) i7-4720HQ CPU on a Windows system. AdaptSky is trained for 1000 episodes with 300 time steps each and tested for 1000 time steps. For simplicity, we only

Algorithm 1: AdaptSky

- 1 Initialize replay memory ζ with capacity M .
- 2 Initialize the policy network Q with random weights and biases θ^π .
- 3 Clone the policy network Q weights and biases to the target network $Q' \rightarrow \theta'^\pi = \theta^\pi$.
- 4 **for** $episode = 0, 1, \dots, (E - 1)$ **do**
- 5 Initialize the UAV environment: receive the starting state s_0 and pre-processed state $\phi_0 = \phi(s_0)$.
- 6 **for** $\tau = 0, 1, \dots, (T - 1)$ **do**
- 7 Select a random action a_τ with probability ϵ (Exploration): Choose a random action
 Otherwise (Exploitation) select a_τ by passing $\phi(s_\tau)$ to the policy network and choose $\arg \max_{a_\tau} Q(\phi(s_\tau), a_\tau; \theta^\pi)$
- 8 Execute a_τ .
- 9 Observe reward r_τ and next state $s_{\tau+1}$.
- 10 Set $s_\tau = s_{\tau+1}$ and pre-process $\phi_{\tau+1} = \phi(s_{\tau+1})$
- 11 Store experience $(\phi_\tau, a_\tau, r_\tau, \phi_{\tau+1})$ in ζ .
- 12 Sample random mini-batch of experiences from ζ .
- 13 Pass the mini-batch to the policy network and observe the output Q-values of $Q(\phi_\tau, a_\tau; \theta^\pi)$.
- 14 Pass $s_{\tau+1}$ mini-batch to the target network Q' .
- 15 Observe the output Q-values of the next states.
- 16 Choose the target Q-values
 $\rightarrow Q' = \max Q'(\phi_{\tau+1}, a_{\tau+1}; \theta'^\pi,)$.
- 17 Calculate the loss $L(\theta^\pi)$ between output Q-values $Q(\phi_\tau, a_\tau; \theta^\pi)$ and target Q-values $Q'(\phi_{\tau+1}, a_{\tau+1}; \theta'^\pi,)$ as in equation (13).
- 18 Updates weights and biases θ^π in the policy network that minimize loss $L(\theta^\pi)$ using Gradient descent.
- 19 Update weights and biases in the target network to the weights and biases of the policy network $\theta'^\pi = \theta^\pi$ after δ time steps.

consider large scale fading and intend to study small scale fading and time-variability in our future work. We compare our finding with the state-of-art technique in [6] which throughout the section will be referred to as SoA. For evaluation, we consider \bar{R}_e^{tot} as the average sum-rate achieved per episode. It is determined by averaging the average rate per episode over the most recent 100 episodes. Before that, the moving average is set to zero.

1) Performance of AdaptSky in the sub-6GHz spectrum:

Data rate in generic channel condition. We show in Fig. 2, \bar{R}_e^{tot} for both cases where users-UAV links are dominated by LoS and the case where the channel is generic (LoS and NLoS exist) and compare to SoA which only works for LoS scenario. The simulations have been conducted for 10 runs and the average and the confidence interval of 1 standard deviation have been calculated and plotted as shown in Fig. 2. AdaptSky tends to adapt the power allocation and UAV placement

TABLE I: Network parameters value.

Parameter	mmWave	sub-6GHz
Carrier Frequency (GHz)	28	2
Transmit power(P_T)	20 dBm	30 dBm
Antenna configurations ($\mathcal{N}_{\text{UAV}} \times \mathcal{N}_{\text{UE}}$)	[8, 8]	[1, 1]
System bandwidth (W)	2 GHz	50 MHz
Thermal noise (σ^2)	-84 dBm	-88 dBm
Urban LOS probability parameter (C, b)	9.6117	0.6
Urban LOS probability parameter (Y, s)	0.1581	0.11
Path loss intercept (C_{LoS})	$10^{-6.4}$	-
Path loss intercept (C_{NLoS})	$10^{-7.2}$	-
Mean additional LoS path loss (η_{LoS})	-	1 dB
Mean additional NLoS path loss (η_{NLoS})	-	20 dB
Path loss exponent (a_{LoS})	2	-
Path loss exponent (a_{NLoS})	2.92	-
Minimum elevation angle (θ_0)	-	15°

continuously such that \bar{R}_e^{tot} keeps improving until it converges to a certain value. Furthermore, AdaptSky outperforms SoA despite the fact that AdaptSky is allocating resources in a more complex environment. In LoS scenario, we set $w_r = 1, w_f = 0, w_l = 10^7$, and $w_m = 0$, while in the generic scenario we set $w_f = 5$ so that we prevent the UAV from favoring one user while ignoring the others (since it is the best way to achieve high sum rate with the existence of NLoS users). Not only AdaptSky achieves a high fairness level of 60%, but also a \bar{R}_e^{tot} , that converges to 400 Mbps which is 163% higher than that achieved by the SoA. Although it is not reasonable to compare AdaptSky to SoA with the presence of NLoS users since SoA has only LoS users, AdaptSky achieves a better \bar{R}_e^{tot} and maintains a 40% fairness level even though the NLoS results approximately in two orders of magnitude worse path loss.

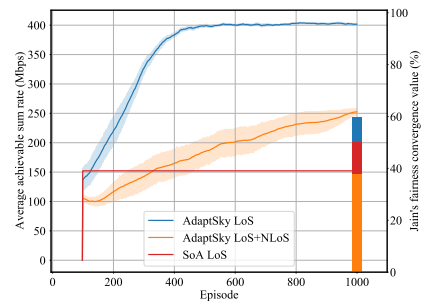


Fig. 2: AdaptSky sub-6GHz performance in several scenarios compared to the state-of-art.

2) *AdaptSky for mmWave-NOMA-UAV Networks:* We evaluate AdaptSky performance in terms of training and testing processes for different scenarios.

Training process. Assuming that the channels are only LoS, throughout this analysis, we train AdaptSky to allocate resources by maximizing total average data rate while satisfying the minimum spectral efficiency specified by R_{min}/W . To satisfy the stated objective and constraint we set w_f & w_l to be zero and w_m to be 100. In Fig. 3, we plot \bar{R}_e^{tot} as a function of the minimum spectral efficiency. Observe that AdaptSky has a superior performance than SoA, thanks to moving in the 3D plane while allocating power at the same time. Also, observe that AdaptSky maintains a spectral efficiency up to 3 bit/s/Hz

to all the users while SoA can only handle up to 2.5 bit/s/Hz. **Testing process.** Now, we examine the effectiveness and

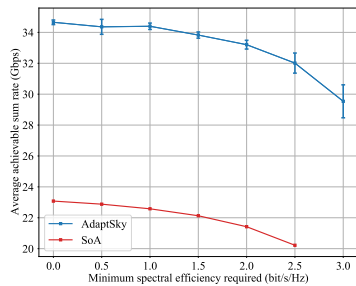


Fig. 3: Average achievable sum rate as function of minimum spectral efficiency required in mmWave.

robustness of AdaptSky when implemented using DRL and DN-DRL with uniform random distribution of the UEs. Fig. 4 confirms previous observation as in 74% of locations, DRL-based AdaptSky significantly outperforms SoA. More interestingly, DN-DRL-based AdaptSky shows even more robustness in terms of generalization and it outperforms DRL-based AdaptSky by 68%.

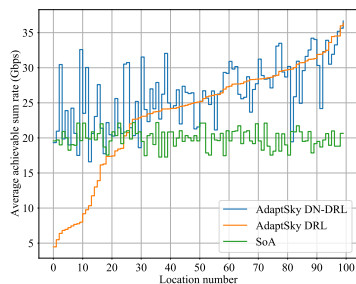


Fig. 4: Average achievable sum rate for different users location in mmWave.

the power allocation and UAV placement and restricting the UAV to 2D location does lead to inefficient use of resources. Hence, these simulation results demonstrate the significant advantage of our proposed framework over the state-of-the-art, by unleashing the power of AI and the importance of solving the power allocation and the 3D-UAV placement jointly.

VI. CONCLUSION

In this paper, we proposed AdaptSky, a novel AI-based framework built based on deep reinforcement learning with DN architectures, and used for resource allocation and UAV placement. AdaptSky optimizes a UAV 3D location while allocating resources effectively in NOMA-UAV networks, simultaneously, for a generic-realistic path loss. Simulation results showed that AdaptSky yields significant performance gains over conventional approaches in terms of achievable sum rate in many different scenarios both in training and testing.

REFERENCES

- [1] Shuping Dang, Osama Amin, Basem Shihada, and Mohamed-Slim Alouini. What should 6G be? *Nature Electronics*, 3(1):20–29, 2020.
- [2] Khaled B Letaief, Wei Chen, Yuanming Shi, Jun Zhang, and Ying-Jun Angela Zhang. The roadmap to 6G: AI empowered wireless networks. *IEEE Communications Magazine*, 57(8):84–90, 2019.
- [3] Mostafa Zaman Chowdhury, Md Shahjalal, Shakil Ahmed, and Yeong Min Jang. 6G wireless communication systems: Applications, requirements, technologies, challenges, and research directions. *IEEE Open Journal of the Communications Society*, 1:957–975, 2020.
- [4] Xingqin Lin, Vijaya Yajnanarayana, Siva D Muruganathan, Shiwei Gao, Henrik Asplund, Helka-Liina Maattanen, Mattias Bergstrom, Sebastian Euler, and Y-P Eric Wang. The sky is not the limit: LTE for unmanned aerial vehicles. *IEEE Communications Magazine*, 56(4):204–210, 2018.
- [5] Yuanwei Liu, Zhijin Qin, Yunlong Cai, Yue Gao, Geoffrey Ye Li, and Arumugam Nallanathan. UAV communications based on non-orthogonal multiple access. *IEEE Wireless Communications*, 26(1):52–57, 2019.
- [6] Xiaonan Liu, Jingjing Wang, Nan Zhao, Yunfei Chen, Shun Zhang, Zhiguo Ding, and F Richard Yu. Placement and power allocation for NOMA-UAV networks. *IEEE Wireless Communications Letters*, 8(3):965–968, 2019.
- [7] Pankaj K Sharma and Dong In Kim. UAV-enabled downlink wireless system with non-orthogonal multiple access. In *2017 IEEE Globecom Workshops (GC Wkshps)*, pages 1–6. IEEE, 2017.
- [8] Fangyu Cui, Yunlong Cai, Zhijin Qin, Minjian Zhao, and Geoffrey Ye Li. Joint trajectory design and power allocation for UAV-enabled non-orthogonal multiple access systems. In *2018 IEEE Global Communications Conference (GLOBECOM)*, pages 1–6. IEEE, 2018.
- [9] Mehdi Monemi, Hina Tabassum, and Ramein Zahedi. On the performance of non-orthogonal multiple access (NOMA): Terrestrial vs. aerial networks. In *2020 IEEE Eighth International Conference on Communications and Networking (ComNet)*, pages 1–8, 2020.
- [10] Hajar El Hammouti, Mustapha Benjillali, Basem Shihada, and Mohamed-Slim Alouini. Learn-as-you-fly: A distributed algorithm for joint 3d placement and user association in multi-UAVs networks. *IEEE Trans. on Wireless Communications*, 18(12):5831–5844, 2019.
- [11] Mohamed Alzenad, Amr El-Keyi, Faraj Lagum, and Halim Yanikomeroglu. 3-d placement of an unmanned aerial vehicle base station (UAV-bs) for energy-efficient maximal coverage. *IEEE Wireless Communications Letters*, 6(4):434–437, 2017.
- [12] R Irem Bor-Yaliniz, Amr El-Keyi, and Halim Yanikomeroglu. Efficient 3-d placement of an aerial base station in next generation cellular networks. In *2016 IEEE international conference on communications (ICC)*, pages 1–5. IEEE, 2016.
- [13] Volodymyr Mnih, Koray Kavukcuoglu, David Silver, Alex Graves, Ioannis Antonoglou, Daan Wierstra, and Martin Riedmiller. Playing atari with deep reinforcement learning. *arXiv preprint:1312.5602*, 2013.
- [14] Volodymyr Mnih, Koray Kavukcuoglu, David Silver, Andrei A Rusu, Joel Veness, Marc G Bellemare, Alex Graves, Martin Riedmiller, Andreas K Fidjeland, Georg Ostrovski, et al. Human-level control through deep reinforcement learning. *nature*, 518(7540):529–533, 2015.
- [15] Chi Harold Liu, Zheyu Chen, Jian Tang, Jie Xu, and Chengzhe Piao. Energy-efficient UAV control for effective and fair communication coverage: A deep reinforcement learning approach. *IEEE Journal on Selected Areas in Communications*, 36(9):2059–2070, 2018.
- [16] Akram Al-Hourani, Sithamparanathan Kandeepan, and Simon Lardner. Optimal lap altitude for maximum coverage. *IEEE Wireless Communications Letters*, 3(6):569–572, 2014.
- [17] Mustafa Riza Akdeniz, Yuanpeng Liu, Mathew K Samimi, Shu Sun, Sundeepr Rangan, Theodore S Rappaport, and Elza Erkip. Millimeter wave channel modeling and cellular capacity evaluation. *IEEE journal on selected areas in communications*, 32(6):1164–1179, 2014.
- [18] Akram Al-Hourani, Sithamparanathan Kandeepan, and Abbas Jamalipour. Modeling air-to-ground path loss for low altitude platforms in urban environments. In *2014 IEEE global communications conference*, pages 2898–2904. IEEE, 2014.
- [19] Mohamed M El-Sayed, Ahmed S Ibrahim, and Mohamed M Khairy. Power allocation strategies for non-orthogonal multiple access. In *2016 International Conference on Selected Topics in Mobile & Wireless Networking (MoWNeT)*, pages 1–6. IEEE, 2016.
- [20] Rajendra K Jain, Dah-Ming W Chiu, William R Hawe, et al. A quantitative measure of fairness and discrimination. *Eastern Research Laboratory, Digital Equipment Corporation, Hudson, MA*, 1984.
- [21] Leslie Pack Kaelbling, Michael L Littman, and Andrew W Moore. Reinforcement learning: A survey. *Journal of artificial intelligence research*, 4:237–285, 1996.

- [22] Zijun Zhang. Improved adam optimizer for deep neural networks. In *2018 IEEE/ACM 26th International Symposium on Quality of Service (IWQoS)*, pages 1–2. IEEE, 2018.
- [23] Ziyu Wang, Tom Schaul, Matteo Hessel, Hado Hasselt, Marc Lanctot, and Nando Freitas. Dueling network architectures for deep reinforcement learning. In *International conference on machine learning*, pages 1995–2003. PMLR, 2016.